

1 **Cover Page**

2 **Comparative analysis of mammal genomes unveils key genomic variability for human**
3 **lifespan.**

4 **Authors:** Farré X.¹, Molina R.², Barteri F.¹, Timmers P.R.H.J.^{3,4}, Joshi P.K.⁴, Oliva B.²,
5 Acosta, S.¹, Esteve-Altava B.¹, Navarro A.^{1,5,6,7*}, Muntané G.^{1,8*}

6

7 ¹ Institute of Evolutionary Biology (UPF-CSIC), Department of Experimental and Health
8 Sciences, Universitat Pompeu Fabra, Barcelona, Spain

9 ² Structural Bioinformatics Lab, Department of Experimental and Health Sciences,
10 Universitat Pompeu Fabra, 08003, Barcelona, Spain.

11 ³ MRC Human Genetics Unit, MRC Institute of Genetics & Molecular Medicine, University of
12 Edinburgh, Edinburgh, UK

13 ⁴ Centre for Global Health Research, Usher Institute, University of Edinburgh, Edinburgh
14 EH8 9AG, Scotland, UK.

15 ⁵ BarcelonaBeta Brain Research Center (BBRC), Pasqual Maragall Foundation, Wellington
16 30, 08005, Barcelona, Spain.

17 ⁶ Centre for Genomic Regulation (CRG), The Barcelona Institute of Science and Technology,
18 Barcelona, Spain

19 ⁷ Institució Catalana de Recerca i Estudis Avançats (ICREA), Pg. Lluís Companys 23, 08010
20 Barcelona, Spain.

21 ⁸ Hospital Universitari Institut Pere Mata, IISPV, Universitat Rovira i Virgili, Biomedical
22 Network Research Centre on Mental Health (CIBERSAM), Reus, Spain

23

24 **Institution at which research was done:** Institut Biologia Evolutiva, Department of
25 Experimental and Health Sciences, Universitat Pompeu Fabra - CSIC, Barcelona 08003,
26 Spain

27

28 ***Corresponding authors:**

29 Arcadi Navarro (arcadi.navarro@upf.edu)

30 Gerard Muntané (gerard.muntane@upf.edu, muntaneg@peremata.com)

31 **Abstract**

32 Mammals vary 100-fold in their maximum lifespan. This enormous variation is the result of
33 the adaptations of each species to their own biological trade-offs and ecological conditions.
34 Comparative genomics studies have demonstrated that the genomic factors underlying the
35 lifespans of species and the longevity of individuals are shared across the tree of life. Here,
36 we set out to compare protein-coding regions across the mammalian phylogeny, aiming to
37 detect individual amino acid changes shared by the most long-lived mammal species and
38 genes whose rates of protein evolution correlate with longevity. We discovered a total of
39 2,737 amino acid changes in 2,004 genes that distinguish long- and short-lived mammals,
40 significantly more than expected by chance ($p=0.003$). The detected genes belong to
41 pathways involved in regulating lifespan, such as inflammatory response and hemostasis.
42 Among them, a total 1,157 amino acids, located in 996 different genes, showed a significant
43 association with maximum lifespan in a phylogenetically controlled test. Interestingly, most of
44 the detected amino acids positions do not vary in extant human populations (>81.2%) or
45 have allele frequencies below 1% (99.78%), Consequently, almost none could have been
46 detected by Genome-Wide Association Studies (GWAS). Additionally, we identified four
47 more genes whose rate of protein evolution correlated with longevity in mammals. Crucially,
48 SNPs located in the detected genes explain a larger fraction of human lifespan heritability
49 than expected by chance, successfully demonstrating for the first time that comparative
50 genomics can be used to enhance the interpretation of human GWAS. Finally, we show that
51 the human longevity-associated proteins coded by the detected genes are significantly more
52 stable than the orthologous proteins from short-lived mammals, strongly suggesting that
53 general protein stability is linked to increased lifespan.

54 **Introduction**

55 Why some individuals within a species live longer than others is intimately related to the
56 broader question of why some species live longer than others (Tian, Seluanov, and
57 Gorbunova 2017). Maximum lifespan (MLS) is a species-specific trait: flies, dogs, and
58 humans all have different but consistent lifespans that are adapted to their ecology and
59 biology. From an evolutionary standpoint, the main ultimate cause of these differences are
60 lineage-specific ecological adaptations that modify the rates of extrinsic mortality. For
61 instance, lifespan is usually lengthened by arborealism (Shattuck and Williams 2010), flight
62 (Pomeroy 1990), subterranean life (Buffenstein 2005), and body mass (Austad 2005; de
63 Magalhães, Costa, and Church 2007) since all these adaptations reduce extrinsic mortality
64 by predation. Most of these differences and similarities in MLS are explained by common
65 physiological, biochemical, and genetic basis across species (Ma and Gladyshev 2017).

66 Mammals show a 100-fold variation in MLS, ranging from short-lived species like forest
67 shrews (~2 years) to long-lived species like the bowhead whale (~200 years, Tacutu et al.
68 2018), representing an ideal lineage to study the genomics of lifespan and to unveil genes
69 and pathways that may be relevant for humans. Numerous studies have been devoted to
70 study mammal lifespan focusing on individual species, such as the bowhead whale (Keane
71 et al. 2015) and the naked mole rat (Kim et al. 2011; Ruby, Smith, and Buffenstein 2018), or
72 relatively small subgroups like bats (Huang et al. 2019; Wang et al. 2020; Seim et al. 2013).
73 While single-species studies have yielded some credible candidate genes associated with
74 increased lifespan, it is difficult to obtain generalizations on universal mechanisms of lifespan
75 regulation from them. Therefore, knowledge about lifespan evolution in mammals is still
76 limited. Our mammalian ancestors, although diverse (Pickrell 2019), were small (O'Leary et
77 al. 2013), and in all likelihood short-lived creatures. Whereas the long-term directional bias
78 towards increasing size in mammals (Baker et al. 2015; Lyson et al. 2019) could drive a
79 parallel trend towards increased lifespan, there is no strong evidence in favor of that
80 hypothesis.

81 Other comparative genomics studies have focused on identifying rapid evolutionary changes
82 in genomes or transcriptomes that correlate with changes in longevity (Kim et al. 2011;
83 Muntané et al. 2018; Kowalczyk et al. 2020); or have assessed the relationship between
84 lifespan and other adaptations with life-history traits in different taxa (Montgomery and
85 Mundy 2012; Boddy et al. 2017; Wang et al. 2020; Zhang et al. 2014; Chikina, Robinson,
86 and Clark 2016; Foote et al. 2015). These studies have identified longevity pathways that
87 are conserved across species, such as the insulin/IGF-1 pathway, telomere maintenance,
88 DNA repair, coagulation and wound healing, proteostasis, and TOR signaling. The existence

89 of such common pathways and mechanisms is consistent with the fact that long-lived
90 animals show convergent phenotypes, including increased stress resistance, altered
91 metabolism, and delayed reproduction and development (Hekimi 2003).

92 A key mechanism that may contribute to differences in lifespan is the maintenance of the
93 proteostasis network. Protein stability or proteostasis refers to the capacity to protect protein
94 structures and functions against environmental stressors, including aging. In fact,
95 dysfunction of the protein quality control mechanisms is a hallmark of aging (López-Otín et
96 al. 2013; Santra, Dill, and de Graff 2019) and there is substantial evidence linking
97 proteostasis and longevity (reviewed in Tian, Seluanov, and Gorbunova 2017). For instance,
98 improved protein stability is determinant for longevity in exceptionally long-lived mollusks
99 (Treaster et al. 2014) and in the naked mole-rat, the longest-living rodent (Pérez et al. 2009).
100 In addition, interventions that enhance proteome stability can improve health or increase
101 lifespan in model organisms (Fontana and Partridge 2015), such as pharmacological
102 chaperones that have been investigated as potential therapeutic targets to reduce the
103 adverse effects of. misfolding of aging-related proteins (Powers et al. 2009; Bullock et al.
104 1997).

105 Despite of all the evidence outlined above, a mammalian-wide study of the genomic
106 underpinnings of lifespan has never been carried out with the combined goals of identifying
107 individual mutations linked to longevity; analyzing the functional properties of their genes and
108 the pathways in which they take part; and studying how the stability of the proteins coded by
109 these genes may differentiate long- and short- lived species. In fact, the largest-scale studies
110 conducted on mammalian lifespan have focused only on humans, with somewhat limited
111 results (e.g., Timmers et al. 2019). The low heritability of lifespan in humans may explain
112 these limitations. Studies in twins have reported values of heritability between 0.2 and 0.3
113 (Herskind et al. 1996; Sebastiani and Perls 2012). More recently, the analysis of family trees
114 produced an estimation of around 0.1, suggesting that previous estimates were inflated due
115 to assortative mating (Kaplanis et al. 2018; Ruby et al. 2018). Several GWAS on human
116 lifespan have been carried out using different indirect measures and strategies, such as
117 parental lifespan (Timmers et al. 2019), extremely long lived individuals (Deelen et al. 2019),
118 or health span (Zenin et al. 2019). While these studies have identified a set of genetic
119 variants that are associated with an individual's lifespan, only a small fraction of the
120 heritability –around 5%– has been disclosed by GWAS. In summary, not only we are missing
121 important contributions to extant human variation on lifespan, probably due to genetic
122 variants with small effects (de Magalhães and Wang 2019; Muntané et al. 2018); but also,

123 and given the relatively small genetic variation in lifespan in our species, we still lack a map
124 of the full landscape of genomic factors underlying lifespan.

125 Here, we performed the largest phylogeny-based genome-phenome analysis to date,
126 focusing on the detection of individual mutations and genes that underlie the enormous
127 variation of lifespan in mammals. We report the discovery of more than 2,000 longevity-
128 related genes and show that, overall, they present a trend towards increased protein stability
129 in long-lived organisms. In addition, we successfully show that our findings enhance the
130 interpretation of the results of lifespan GWAS that have been carried-out in humans.
131 Altogether, our results pave the way for the use of comparative genomics studies to shed
132 light on human traits, particularly those of potential medical interest.

133 **Materials and Methods**

134 Genomic and phenotypic data

135 Amino acid (AA) and nucleotide alignments for 39,178 orthologous coding sequences were
136 retrieved from the Multiz alignment of 100 vertebrate genomes (Human 100-way) together
137 with the mammalian phylogenetic tree, which was also downloaded from UCSC
138 (<https://genome.ucsc.edu/>, last accessed August 2019). Amongst the 100 vertebrate
139 species, we kept the 62 species belonging to the class Mammalia (Supplementary Figure 1).
140 For each gene, only the longest transcript was kept and protein alignments with an overall
141 number of gaps > 50% or in human alternate contigs were excluded (n=905). After this
142 filtering, a total of 18,266 protein transcripts were included in the analyses.

143 Variation in MLS across species correlates with many life-history traits, including body mass,
144 growth rate, age at sexual maturity, and body temperature, which can bias comparative
145 studies of lifespan (Speakman 2005). The most relevant and studied confounding factor is
146 body mass, so longevity is usually corrected by it using the longevity quotient (LQ), which
147 indicates whether a species has an average lifespan or is unusually long- or short-lived
148 relative to its body size. LQs is computed as the ratio of a species MLS to the expected MLS
149 given its body mass (Austad and Fischer 1991). MLS and adult body mass were obtained
150 from the AnAge database (Tacutu et al. 2018, build 14) and missing information was
151 complemented, when available, using data from the Animal Diversity Web (Myers et al.
152 2019). The LQ of each species was calculated using the allometric equation for mammals
153 (de Magalhães, Costa, and Church 2007). After filtering out species for those we were
154 unable to obtain LQ data, we kept a final number of 57 mammalian species for subsequent
155 analyses (Supplementary Figure 1 and Supplementary Table 1).

156 Convergent Amino Acid Substitutions: Discovery and Validation

157 Convergent amino acid substitutions (CAAS) are AA changes that have occurred
158 independently at least twice across the phylogeny. For the purposes of this work, we
159 focused on CAAS that coincide with extreme lifespan values in the set of mammalian
160 species under study. We designed a two-phase procedure to identify such instances of
161 CAAS. First, in the *Discovery phase*, we selected the species in the top and low deciles of
162 the LQ distribution, which we named long-lived and short-lived, respectively, for a total of 12
163 extremely lived species (6 top and 6 low). Subsequently, an in-house script was used to
164 detect specific protein positions in which the reference genomes of the long-lived species
165 had the same AA and the short-lived group presented either another AA (Scenario 1) or a
166 set of segregating AAs that were different from the reference AAs in the long-lived-group
167 (Scenario 2). Positions where the short-lived group showed a fixed AA, and where
168 segregating, non-intersecting variation was observed in the long-lived group were also
169 considered (Scenario 3). For the purposes of this work, we only focused on Scenarios 1 and
170 2, representing the AA substitutions converging in the mammal long-lived species
171 (discussed in Supplementary Note). We required full information from all species in the
172 extremes, so AA positions for which one or more of the species had a gap were excluded
173 from the analysis. Such a filter resulted in a final set of 13,035 genes evaluated using the
174 CAAS procedure (Figure 1).

175 To ascertain whether the number of CAAS identified as linked to extremely-lived species
176 groups was different than random expectations, we performed two resampling tests. In both
177 tests, two groups of 6 species were randomly taken from the phylogeny 1,000 times and the
178 procedure to identify CAAS was repeated. The p-value was the empirical probability of
179 getting a number of CAAS equal or larger than the original observation. The two resampling
180 procedures differed in their consideration of the phylogeny. The first resampling was
181 independent of the phylogeny; the species were selected completely at random (*random*
182 *resampling*). The second resampling method was designed to maintain the same proportion
183 of species in each order as those in the observed data (*guided resampling*). For mammalian
184 orders where there were no other species to resample, we were conservative and always
185 included the same species.

186 The second phase, a *Validation phase*, was applied to each AA pin-pointed in the *Discovery*
187 *phase*. It consisted in validating whether the species in the intermediate deciles (middle 80%
188 of the LQ distribution, a total of 45 species) that had the same AA as the long-lived species
189 also had a higher LQ than those species having the same AA change/s as the short-lived
190 species. When short-lived species displayed more than one AA, all of them were included in

191 the Validation phase. However, AA present among the species of the intermediate deciles
192 but that were not observed in the long-lived or the short-lived group, were discarded. For
193 validation, we used a phylogenetic ANOVA test as implemented in the *RRPP* package in R,
194 using 10,000 iterations for significance testing (Collyer and Adams 2018, Figure 1). Finally,
195 to further validate the longevity signal recovered in the gene set we also performed an
196 external validation with another mammal set of species (Supplementary Note).

197 Annotation of CAAS

198 We analyzed the functional effects of the nucleotide changes leading to CAAS, their
199 population frequency in humans and their association to complex diseases. The most likely
200 nucleotide substitutions corresponding to AA substitutions associated with high LQ in
201 mammals were ascertained using the *panno* option from TransVar (Zhou et al. 2015) and
202 visualized in the protein context (Supplementary Note). The frequency of each genetic
203 variant in current human populations was obtained from the GnomAD v3 variant database
204 (Karczewski et al. 2020). In those positions showing variable AA in the short-lived species
205 (Scenario 2), we selected the more conservative option to avoid duplicated sites. That is, we
206 assessed all possible combinations and kept the alternative with the highest allele frequency
207 in humans. Also, those cases in which the most plausible variation leading to the AA
208 mutation implied the change of more than one nucleotide of a codon were excluded from the
209 variation analysis. The same procedure was repeated for 100 random sets of AA
210 substitutions to test whether our observations on genetic variation in the discovered
211 positions fitted the random expectations (Supplementary Note).

212 The functional prediction of the genetic variants, as well as the SIFT and PolyPhen2 scores
213 were obtained from the Variant Effect Predictor (VEP, McLaren et al. 2016). SIFT and
214 PolyPhen2 predict the functional impact of an AA substitution, the first by leveraging the
215 sequence homology and physical properties of the AA (Ng and Henikoff 2003), and the later
216 by using physical and comparative models based on evolutionary conservation and structure
217 (Adzhubei et al. 2010). CADD scores were obtained from the CADD project website
218 (<https://cadd.gs.washington.edu/>, Rentzsch et al. 2019), and used to assess the
219 deleteriousness of genetic variants, by classifying those with a Phred score higher than 30
220 as likely deleterious variants.

221 For the identified positions in Scenario 1, ancestral states were reconstructed to assess the
222 likelihood of the last common ancestor of mammals harboring the putatively long- or short-
223 lived AA. Simulation of the ancestral AA was performed using an empirical Bayes method as
224 implemented in the R package *phytools* (Revell 2012). To avoid cases in which the ancestral

225 AA was uncertain, we only kept those in which the AA in the root of the tree had a probability
226 higher than 0.8. We then quantified the cases in which the ancestral reconstructed AA was
227 the one present in the short-lived or long-lived mammals. Additionally, for Scenario 1
228 substitutions, we simulated 100 stochastic character maps using a fixed transition matrix that
229 assumes the same rate of change for any AA transition to estimate the number of AA
230 changes of each type, in order to quantify the number of changes across the phylogeny from
231 any AA to the long-lived or to the short-lived AA (Huelsenbeck, Nielsen, and Bollback 2003).

232 Protein models

233 We aimed to compare protein energy variations between short- and long-lived mammals.
234 Since *Rattus norvegicus* proteins have been the object of numerous studies, we selected
235 that species as the representative of short-lived group of mammals in our analysis. Humans
236 were selected as long-lived representatives. Not all proteins had known structures for both
237 organisms. Out of 104 protein sequences in which we have discovered CAAS and that have
238 known structures, we only found 40 protein sequence-pairs with high similarity and validated
239 CAAS, from both human and rat. Then, we used MODELLER (Webb and Sali 2016) to
240 model both structures of the pair, using the structures of the known templates and the
241 sequence alignments obtained with “matcher” (from EMBOSS package) (Rice, Longden, and
242 Bleasby 2000). The modelled structures were optimized with the repair-pdb protocol from
243 FoldX (Buß, Rudat, and Ochsenreither 2018). We used the optimized structures to calculate
244 the differences of Fold X energies (ΔE) between the human and rat protein sequences.

245 We selected all the sequences of *Rattus norvegicus* available in Uniprot with known 3D
246 structure (n=667) as a background set to compare the ΔE distributions of proteins coded by
247 genes harboring CAAs with the distributions of ΔE s of pairs of sequences from genes
248 without CAAS. After removing the ones in the set with CAAS described in the previous
249 paragraph, we obtained 337 structural models of highly similar human sequences. Note that
250 we were not able to model the structure of all proteins due to threading mismatches. Outliers
251 were removed from both distributions by generating an Interquartile Range (IQR) with a
252 weigh of 4: $IQR = 4 * (\text{upper quartile} - \text{lower quartile})$. The distribution was normalized by the
253 maximum value to have comparable ranges between 0 and 1. We compared the distribution
254 of the pairs with validated CAAS with the background distribution of non-validated CAAS
255 using a permutation two-sample test (<https://statlab.github.io/permute/user/two-sample.html>).

256 We further tested the robustness of the results by increasing the size of the background. We
257 increased the background with protein-pairs of highly similar human and rat sequences
258 without validated CAAS, selected randomly. After parsing around 4,000 sequences, we

259 obtained 500 pairs of rat-human sequences whose structure could be modelled for both
260 species. We used the same protocol for modelling and optimization of the structures, and the
261 distribution of ΔE s was similarly normalized and analyzed, using a permutation two-sample
262 test for the comparison.

263 Gene-Phenotype Coevolution across mammals

264 The nucleotide alignments that underwent previous quality control (< 50% of gaps) were
265 used for studying the coevolution of genes and phenotype. We estimated root-to-tip rates of
266 protein evolution (the dN/dS ratio or ω) using the free-ratio model from PAML 4.9a (Yang
267 1997). The root-to-tip ω is a property of the species tip rather than of the terminal branch,
268 thus being more inclusive of the evolutionary history of a locus and, therefore, it is more
269 suitable for regressions against phenotypic data from extant species (Montgomery and
270 Mundy 2012). Briefly, for each gene and species we computed the root-to-tip dNs and dSs
271 and the ratio between these values to obtain the root-to-tip ω , as previously described in
272 Muntané et al. 2018. To avoid numerical problems with the log transformation and unrealistic
273 substitution rates, the species for which the root-to-tip ω was 0 were discarded, with 877
274 genes having at least one species removed. Genes for which we could not estimate a root-
275 to-tip value for, at least, half of the species were also removed from further analyses,
276 resulting in a final set of 17,969 genes.

277 For each gene, we studied the association between its rate of protein evolution and longevity
278 regressing root-to-tip ω and LQ by means of phylogenetic generalized least squares (PGLS)
279 as implemented in the *caper* library in R (Orme 2018). PGLS allows to incorporate the
280 phylogenetic relationship among species in the error term of a generalized least squares
281 model, thus controlling for the phylogenetic inertia (close species may have more similar
282 phenotypes than distant species). Pagel's lambda (λ) was estimated through maximum
283 likelihood in each case. Pagel's λ values equal or close to 1 indicate that a character is
284 evolving stochastically (Brownian motion) along the tree, whereas $\lambda \ll 1$ indicates that a
285 character evolution is independent of the phylogeny. In 295 genes, estimations of λ resulted
286 in a value of 0 and the log-likelihood plots showed a flat likelihood surface (for an example,
287 see Supplementary Figure 2), which is most likely due to reduced sample size (DeCasien,
288 Williams, and Higham 2017). Consequently, for these cases we set the value of λ to the
289 genome-wide median λ value. To control for the effect of effective population size covarying
290 with LQ, median genome-wide root-to-tip ω s was included in the PGLS models as covariate
291 (Boddy et al. 2017). Also, species with studentized residuals $> \pm 3$ were considered outliers
292 and, thus, removed from the regression and PGLS was fitted again. Moreover, to control that
293 no single species was biasing the PGLS models, we performed an additional step and

294 repeated regressions: by removing one species at a time and keeping the maximum p-value
295 (p-value conservative). In all regressions, both the LQ and the root-to-tip τ s were log10
296 transformed. Finally, we applied a Benjamini-Hochberg False Discovery Rate (FDR) with an
297 FDR of 5% for multiple test corrections. To avoid associations due to one single species,
298 when we refer to genes that are nominally significant in the PGLS analysis, we always refer
299 to those that were nominally significant for the p-value conservative regressions ($P_{\text{cons}} <$
300 0.05).

301 Functional enrichments

302 To study whether there was an over- or under-representation of genes previously related to
303 aging in our gene sets we used hypergeometric tests. We included lists of genes that had
304 been previously associated with aging (Supplementary Note). Biological mechanisms
305 underlying CAAS were evaluated with WebGestalt, that allows checking for pathway over-
306 representation of specific GO terms, pathways, and disease-associated genes from
307 GLAD4U (Liao et al. 2019). For each evaluated gene set, FDR was controlled using the
308 Benjamini-Hochberg procedure and the set of evaluated genes ($n=13,035$ genes) was used
309 as the background. PGLS results were filtered keeping only those genes that were nominally
310 significant ($P_{\text{cons}} < 0.05$) and then ranked by the t-statistic obtained in the PGLS analysis,
311 subsequently Gene Set Enrichment Analysis (GSEA), from WebGestalt, was carried out to
312 study enriched categories in genes with both a positive and a negative association between
313 root-to-tip τ and LQ.

314 Human lifespan GWAS heritability enrichment

315 To test whether the genes obtained from our comparative analyses could explain genetic
316 variation in human lifespan, LD-score regression (LDSC) was used (Finucane et al. 2015).
317 Specifically, we tested whether both, the genes with CAAS (discovered and validated) and
318 those nominally significant after the PGLS regression, explained a larger fraction of SNP
319 heritability in a human lifespan GWAS than would be expected by chance. Briefly, SNPs on
320 the GWAS of parental lifespan (Timmers et al. 2019) were assigned to genes by annotating
321 and keeping only SNPs in genic regions plus a window of 5kb around each gene.
322 Subsequently, the custom annotation file for LDSC was prepared for five categories: (i) all
323 genic SNPs, (ii) SNPs that map into the genes that were evaluated, (iii) SNPs located in the
324 genes containing discovered CAAS, and (iv) SNPs in the genes harboring phylogenetically
325 validated CAAS and (v) SNPs in the genes that were significant ($P_{\text{cons}} < 0.05$) in the PGLS
326 genome-phenome analysis. Enrichment in human lifespan heritability was evaluated in the
327 detected genes (cat. iii, iv and v) compared heritability explained by the genes evaluated

328 (cat. ii). To help in visualizing the results, stratified QQ-plots were also performed with the
329 SNPs in the five categories.

330 Pathway Scoring Algorithm (PASCAL) is a software that allows testing if a given gene set (or
331 pathway) is enriched in GWAS signal (Lamparter et al. 2016). With this aim, we computed
332 gene scores by aggregating, using the sum of chi-squared option (SOCS), SNP p-values
333 from the GWAS on parental lifespan (Timmers et al. 2019), while correcting for linkage
334 disequilibrium data. These computed gene-based scores were then aggregated across sets
335 of related genes with the pathway analysis tools in PASCAL to obtain a pathway score.
336 Pathway enrichment was evaluated using the chi-squared method. With the aim of testing
337 whether our identified genes were enriched in human lifespan GWAS signal, we built custom
338 pathways using the genes resulting from our analyses (the five categories aforementioned)
339 and computed pathway scores for them. For all of them, we kept only genic regions including
340 a window of 5kb around each gene.

341 Results

342 Convergent Amino Acid Substitutions: Discovery and Validation

343 To detect convergent AA substitutions (CAAS) shared between long-lived mammals, we split
344 species into two groups selecting those in the extreme deciles of the LQ distribution
345 (rounding up to 6 species in each group, Supplementary Figure 1). Throughout the
346 manuscript we used the term “Convergent” rather than “Parallel” AA Substitutions to
347 acknowledge that we cannot guarantee that each substitution had appeared independently
348 in each species. In a first phase, the Discovery phase, we counted all AA changes in which
349 the same AA was present in the reference genomes of the long-lived species, while the
350 short-lived species presented either (i) a different fixed AA (Scenario 1) or (ii) variable AA
351 different from the one in the long-lived group (Scenario 2). The species included in the
352 Discovery phase were three Chiroptera (*Myotis lucifugus*, *Myotis davidii*, and *Eptesicus*
353 *fuscus*), one Rodentia (*Heterocephalus glaber*), and two Primates (*Homo sapiens* and
354 *Nomascus leucogenys*) in the long-lived group, and two Soricomorpha (*Condylura cristata*
355 and *Sorex araneus*), two Rodentia (*Rattus norvegicus* and *Mesocricetus auratus*), one
356 Didelphimorphia (*Monodelphis domestica*), and one Artiodactyla (*Pantholops hodgsonii*) in
357 the short-lived group (See Figure 1 and Supplementary Table 1). Since gaps were not
358 accepted in any of the sequences, the number of genes that were screened for the CAAS
359 discovery was reduced to 13,035. We scanned all the aligned positions finding a total of
360 2,737 CAAS in 2,004 genes: 284 belonged to Scenario 1, and 2,453 to Scenario 2. We also
361 identified 533 CAAS belonging to Scenario 3 (Table 1). It is worth noting that CAAS
362 discovered in Scenario 2 were 4.6 times more frequent than CAAS in Scenario 3. If AA
363 changes occur at random, the difference in the number of discoveries in Scenarios 2 and 3
364 is very unlikely (chi-squared $P=1.88e-270$), which constitutes strong evidence for an
365 evolutionary trend to increased lifespan in the mammalian lineage.

366 We performed two different resampling tests to evaluate if the number of detected CAAS
367 was higher than expected by chance: either randomizing species independently of their
368 phylogenetic relation or randomizing only within mammalian orders (*random* and *guided*
369 resampling, see Methods). The probability of randomly obtaining a number of CAAS equal or
370 higher than the observed one was 0.003 in both resampling tests (Supplementary Figure 3),
371 showing that our set of genes contains a statistical excess of CAAS and that, it is enriched
372 with AA substitutions and genes linked to mammalian longevity after correcting by body
373 mass. In our dataset, the *Didelphimorphia* and *Soricomorpha* orders only contained two and
374 one species, respectively, and so the same species (i.e., *Monodelphis domestica*, *Condylura*
375 *cristata* and *Sorex araneus*) were always included in the *guided* resampling, which resulted

376 in a conservative test.

377 In the Validation phase, we confirmed the discovered CAAS using the species in the
378 intermediate deciles of the LQ distribution. First, we divided them into two groups, those with
379 the same AA as the long-lived species and those with the same AA combination as the
380 short-lived species (Figure 1). Second, we tested whether the group presenting the long-
381 lived AA showed significantly higher LQ using the phylogenetic ANOVA implemented in
382 RRPP. Out of the 2,737 CAAS from Scenarios 1 and 2, we validated a total 1,157 that
383 belong to 996 genes (Table 1 and Supplementary Figure 4). This resulted in a 42.1%
384 validation out of the discovered CAAS (for a discussion on discovery and validation at other
385 thresholds see Supplementary Note). Also, out of the 533 CAAS in Scenario 3, we validated
386 185 (34.7%) that belong to 182 genes. The list of all discovered and validated genes can be
387 found in Supplementary Table 2. We should point out that for some cases the validation test
388 was underpowered, as for some comparisons there were too few species in one of the two
389 groups, which makes it even more important to validate such a high percentage.

390 Ancestral state reconstructions of the CAAS from Scenario 1 showed that, out of the 88
391 instances that were predicted with > 80% probability (Supplementary Table 3), only in four
392 cases the long-lived AA was the ancestral state, while in the remaining 84 cases, the
393 ancestral AA was the short-lived one (for an example see Supplementary Figure 5). To
394 estimate the number of parallel AA changes in each gene from Scenario 1, we simulated
395 100 stochastic character maps for each AA substitution in the tree (a total of 28,400
396 simulations). We observed that in 79 out of the 284 AA substitutions from Scenario 1 there
397 was an average of less than one change from any AA to the short-lived version, which
398 implies that the short-lived AA was at the root of the tree. In 189 out of the 284 CAAS we
399 observed less than 6 changes from any AA to the short-lived AA, while in 213 of the 284
400 CAAS, we observed less than 6 changes from any AA to the long-lived version, showing that
401 the vast majority of CAAS appeared in parallel (Supplementary Figure 6).

402 We found that amongst the 2,004 discovered genes there was an enrichment of genes
403 upregulated with age (FDR=9.43e-04, Enrichment Ratio (ER) = 1.43) and a depletion of age-
404 downregulated genes (depletion FDR=9.99e-09, ER = 0.51), loss of proteostasis
405 (FDR=1.05e-07, ER=0.26), essential genes (FDR=2.76e-06E-06, ER=0.72), and genes with
406 pLI>0.9 (FDR=5.77e-19, ER=0.63). In contrast, there was no enrichment of genes previously
407 associated with longevity from the GenAge database (Supplementary Table 4). The
408 significant enrichments were conserved in the subset of 996 genes phylogenetically
409 validated (Supplementary Note). Additionally, we studied functional enrichments in both the
410 discovered and validated gene sets with WebGestalt (for a complete list of processes

411 enrichments see Supplementary Table 5). The discovered genes were enriched in GO
412 categories such as acute inflammatory response (FDR=1.99e-03), leukocyte migration
413 (FDR=2.75e-02), and cytokine binding (FDR=2.96e-05), in pathways such as
414 *Staphylococcus aureus* infection (FDR=6.34e-04), and complement and coagulation
415 cascades (FDR=2.72e-03), and human diseases such as gram-negative bacterial infections
416 (FDR=2.09e-07), autoimmune diseases (FDR=7.14e-06), systemic inflammatory response
417 syndrome (FDR=1.17e-04), and Werner Syndrome (FDR=1.85e-03), among many others.
418 Also, we found enrichment in hallmark gene sets (Liberzon et al. 2015) such as IL6 STAT3
419 signaling during acute phase response (FDR=3.70e-05) and blood coagulation cascade
420 (FDR=9.50e-05).

421 Among the 2,004 genes harboring CAAS we found eight genes that have been previously
422 linked with longevity. One example is the *WRN* gene, which plays a critical role in repairing
423 damaged DNA, showing two mutations that differ between long-lived and short-lived
424 mammals. One was from Scenario 1, with two AA clearly differentiating long- and short-live
425 mammals (F1018L) and another from Scenario 2 (N1055S/R/K/I/T). Both mutations were in
426 the RQC domain of the protein, which makes these two mutations good candidates for
427 follow-up studies and experimental validation. Another example is *CASP10*, a gene involved
428 in the activation cascade of caspases responsible for apoptosis execution, showed 6 CAAS,
429 all of them located in the caspase domain and validated with the phylogenetic test
430 (Supplementary Figure 7). A final example, *ZC3HC1*, which has been recently identified in
431 the GWAS of parental lifespan (Timmers et al. 2019), contained a validated Scenario 2
432 substitution (T366S/A).

433 Human variation in CAAS

434 Translating CAAS nucleotide changes from short-lived mammals to humans using TransVar,
435 we found 2,704 out of the 2,737 CAAS mapped to a single nucleotide substitution. We
436 excluded the remaining 33 CAAS because they needed more than one nucleotide
437 substitution. We identified human genetic variation in only 516 out of the 2,704 CAAS (19%),
438 but only in 6 cases (0.22%) the minor allele frequency (MAF) was higher than 1%
439 (Supplementary Table 6). This suggests that the vast majority of the identified AA
440 substitutions are fixed or almost fixed (99.78%) in humans and, thus, that they may
441 correspond to genomic factors contributing to lifespan or related traits that are invisible to
442 analyses that exploit variation in current human populations (e.g., GWAS). This observation
443 is much lower than that expected by randomly selecting 100 subsets of 2,737 AA
444 substitutions among the substituted positions between human and rat, and between human
445 and green monkey (empirical $P < 0.01$ in both). In the randomization we observed a mean

446 percentage of 22.4% and 32.85% human genetic variation in the 100 subsets, respectively,
447 and in all simulations the percentage was higher than the observed 19%. Moreover, the
448 number of nucleotide substitutions with a MAF higher than 1% exhibited a mean of 0.60%
449 and 2.36% and only in one out of the 100 randomizations between human and rat, the mean
450 was lower than the 0.22% of the observed (Supplementary Figure 8).

451 Out of the 2,704 CAAS that mapped to a single nucleotide substitution, SIFT and PolyPhen
452 information was obtained for 2,175. A total of 2,134 and 2,112 of the substitutions were
453 considered benign or tolerated in humans according to PolyPhen and SIFT scores,
454 respectively, with 2,079 being considered benign by both metrics. CADD scores evaluated
455 the 516 variants showing human variation as likely benign (summarized in Supplementary
456 Table 7). This represented, for all the scores, an enrichment of tolerated substitutions
457 compared to 100 random samplings (empirical $P < 0.01$, Supplementary Note).

458 Protein models

459 We compared the FoldX changes of total energy between modelled structures of human and
460 rat sequences in 40 protein pairs with validated CAAS. The difference of energy showed that
461 the genes harboring CAAS code for proteins that are more stable in long-lived mammals
462 (represented by human) than in short-lived organisms (represented by rat). To test whether
463 this trend is general or is a property of longevity-related proteins, we analyzed the energies
464 of all the sequences of *Rattus norvegicus* with known structure and without validated CAAS
465 that had similar human sequences whose structure was either known or could be modelled.
466 The permutation test proved the over stability of human sequences with a P-value of $6.3e-04$
467 (Supplementary Figure 9A). This trend was further validated in a larger background set of
468 about 500 structural models of human and rat sequences, and the significance was
469 preserved with P-value of $4.5e-04$ (Supplementary Figure 9B). In short: the accumulation of
470 longevity-related differences in AA residues between short- and long-lived mammals has
471 resulted in increased stability in these proteins in long-lived organisms. The specific role of
472 these AA residues is unclear, as the variability of local energies of FoldX are not remarkable
473 for any specific partial energy (with the only exception of Van Der Waals clashes).

474 Gene-Phenotype coevolution

475 To identify genes with rates of protein evolution associated with changes in LQ across the
476 mammalian phylogeny, we computed the root-to-tip d for each gene and species and
477 evaluated its association with LQ using PGLS. Among the 18,266 gene alignments, 297

478 were removed because for more than half of the species we were not able to compute a
479 root-to-tip dN/dS, finally evaluating 17,969 protein coding sequences.

480 After FDR correction, in the PGLS analysis, four genes showed a significant association
481 between gene root-to-tip ω and species LQ (Figure 2): *SPAG16* ($P=3.58e-7$, slope=3.14),
482 *TOR2A* ($P = 2.26e-7$, slope=-2.44), *ADCY7* ($P = 1.63e-06$, slope=-2.79), and *CDK12* ($P =$
483 $7.81e-06$, slope=3.92). Among the 4 significant genes, two (*SPAG16* and *CDK12*) showed a
484 positive association between rate of protein evolution and LQ, and the other two showed a
485 negative association (*TOR2A* and *ADCY7*). These associations between the root-to-tip ω
486 and the LQ values in the four genes were strong, since even after applying the p-value
487 conservative method (see Methods), they were still the top four genes in the analysis
488 (Supplementary Table 8). Moreover, 705 genes showed a nominal significant association
489 between rate of protein evolution and LQ ($P_{\text{cons}} < 0.05$).

490 Human lifespan GWAS signal enrichment

491 Finally, we evaluated whether the gene sets obtained in our analyses were enriched in
492 current human lifespan array heritability as estimated from GWAS data. We used data from
493 the largest, UK Biobank-based, study on human parental lifespan GWAS to date (Timmers
494 et al. 2019). We partitioned heritability on the genic fraction of the SNPs using LDSC and
495 observed a 3.4-fold enrichment of explained heritability in the set of genes with CAAS
496 compared to the set of screened genes ($P=3.46e-04$). The enrichment was a 2.6-fold for the
497 phylogenetically validated set ($P=0.06$). While genes with a nominal significant association
498 ($P_{\text{cons}} < 0.05$) between rates of protein evolution and LQ showed a 4.2-fold enrichment in
499 GWAS heritability ($P=0.04$, Supplementary Table 9). Figure 3 shows these enrichments
500 using a stratified Q-Q plot, in which a leftward deflection from the null expectation of the
501 subset of SNPs of interest implies an enrichment in GWAS signal. SNPs in the genes that
502 were screened by the CAAS method did not significantly deviate from the expected p-values
503 since it remained close to the line for all the SNPs from the GWAS. On the other hand, the
504 discovered and validated genes, as well as genes that were nominally significant in the
505 PGLS approach deviate from the null expectation and showed an enrichment on GWAS
506 significant p-values. This enrichment on heritability from the parental lifespan GWAS was
507 also confirmed using PASCAL (Lamparter et al. 2016). A chi-squared p-value of $3.27e-05$
508 was obtained for the gene set comprising discovered genes with CAAS (Supplementary
509 Table 10). The gene set created with the genes resulting from the phylogenetic validation
510 also showed a significant enrichment (chi-squared $P=0.039$). Finally, the set of genes that
511 were significant ($P_{\text{cons}} < 0.05$) after a PGLS between LQ and root-to-tip ω 's also showed
512 significant enrichment (chi-squared $P=8.66e-04$).

513 **Discussion**

514 The largest-scale studies trying to unveil the genomic architecture of lifespan variation,
515 including human GWAS, have focused on single species. As a consequence, these studies
516 cannot detect variation that, while fundamental to define lifespan-related phenotypes, may
517 have been fixed in the lineage of a species and may contribute crucially to differences in
518 longevity across species. Comparative genome-phenome analysis, therefore, is essential to
519 obtain a complete view of the genetic architecture of lifespan, to unveil important longevity-
520 related genes and genomic features, and to understand the evolution of long-lived species.
521 Here, we leverage longevity variation across mammalian species to explore cross-species
522 variation and identify mutations and genes linked to the evolution of lifespan. The genes
523 detected belong to pathways potentially involved in longevity, have an increased protein
524 stability in long-lived species, and capture a significant part of the variance in the lifespan of
525 current human populations explained by GWAS.

526 *Genetic architecture of longevity across mammals*

527 Our comparative analysis discovered 3,270 Convergent Amino-Acid Substitutions (CAAS) in
528 2,314 genes using species in the extreme values of LQ distribution. Among them, 2,737
529 CAAS in 2,004 genes were from cases in which all reference genomes of long-lived species
530 present the same reference AA, while short-lived species always present a different AA. This
531 was a statistical excess of discoveries, emphasizing that our gene set is enriched with
532 lifespan-related genetic variation. Out of the 2,737 discoveries, 1,157 CAAS (a 42.3%) in
533 996 genes were validated using the species in the intermediate deciles with a phylogenetic
534 ANOVA test. The observed 42.3% is much higher than the 5% validation expected by
535 chance, showing, again, that our approach can unveil true longevity signals. Furthermore, it
536 should be noted that in the Validation phase, some of the CAAS could not be validated as
537 there was insufficient statistical power due to the small number of species in one of the two
538 groups.

539 Our results strongly support the use of a comparative genetics approach to inform and
540 complement the interpretation of human lifespan GWAS. First, we observed the enrichment
541 of GWAS signal in stratified QQ-plots of human lifespan. Second, focusing on genes that
542 contain discovered and validated AAs, we evaluated whether the proportion of lifespan
543 heritability that they explain was larger than expected by chance. Third, we analyzed a
544 custom pathway created with the obtained gene sets for enrichment in GWAS by using
545 PASCAL. All resulted in significant enrichments for the lists including genes from the
546 convergent substitutions and the gene-phenotype coevolution analysis. Moreover,
547 comparative genomics is the only way to pinpoint most of the genes we report here, since

548 most of the detected AA changes were fixed or almost fixed in current human populations,
549 with only 5 out of 2,230 substitutions (0.22 %) segregating at MAF > 1%. This is significantly
550 less than what is expected by selecting random SNP across the genome and highlights the
551 fact that variation associated with longevity in mammals is almost all fixed in humans. In
552 sum, we demonstrated that an across-species comparative genomics approach can
553 complement the analysis of the genetic architecture of complex traits like LQ.

554 A number of different biologically significant phenomena (e.g., point mutations and post-
555 translational modifications) can change the folding stability of a protein. Here, we found that
556 the proteins harboring AA changes linked to increased lifespan show increased stability in
557 humans compared to short-lived mammals, represented by rats. The exact cause of
558 increased protein stability cannot be determined from the data collected in this work. Some
559 trends suggest that over stability may be due to the contacts in the hydrophobic core, but
560 results were not significant, with the exception of a reduction in van der Waals clashes. Still,
561 an overall explanation for our findings may be that these proteins have accumulated AA
562 changes resulting in increased resistant to the general proteome destabilization that comes
563 with age. In fact, we also observed a significant depletion of genes linked to loss of
564 proteostasis among the discovered gene set. These observations are consistent with
565 evidence showing that long-lived animals have improved protein stability mechanisms (Kim
566 et al. 2011; Pérez et al. 2009; Treaster et al. 2014). Taken together, this is compelling
567 evidence that a common cross-mammalian mechanism to increase lifespan involves
568 proteome stabilization.

569 In line with this observation, the identified longevity-related set was depleted in essential
570 genes and genes intolerant of loss-of-function variation ($pLI \geq 0.9$). Moreover, the
571 deleteriousness scores of the mutations we discovered were enriched in tolerated
572 substitutions compared to random mutations. This could be explained if lifespan evolves
573 through genes and pathways that are not essential to the organisms, which would be fitting
574 with the considerable evolutionary plasticity of longevity in mammals (Ratikainen and Kokko
575 2019).

576 It is of note that there were only 533 cases in which the long-lived species showed variable
577 AA and the reference genomes in the short-lived species presented the same AA (Scenario
578 3). Assuming randomness, this represents a significant reduction from the 2,453 AAs in
579 Scenario 2 (same AA in all long-lived species, different AAs in the short-lived ones). To the
580 best of our knowledge, this is the first genomic evidence of a trend to increased lifespan in
581 mammals, probably driven by positive selection throughout the mammal clade, which is

582 consistent with the fact that stem mammals were small (O'Leary et al. 2013). This
583 observation was validated by the fact that only a 4.5% of the long-lived variants from
584 Scenario 1 were estimated to be present at the root of the mammalian phylogeny, while in
585 the remaining 95.5% the mammalian ancestor was assigned the short-lived variants. In
586 many cases, for instance, substitutions were present in a long-lived ancestor and are shared
587 by sister species, even if there are no sister species in the top and bottom deciles used in
588 the Discovery phase. However, for most AA changes in Scenario 1 we have been able to
589 validate that long-lived species incorporated the AA mutation multiple times in parallel.
590 These cases are examples of independent mutations that appeared in parallel with lifespan
591 shifts across mammals, as described for other biological adaptations, such as echolocation
592 (Liu et al. 2010) or adaptation to aquatic environments (Foote et al. 2015).

593 *Relevant genes and pathways*

594 Discovered genes were enriched in processes involving immune and inflammatory
595 response, cytokine binding and hemostasis, all of them pathways with well-known
596 relationships with lifespan (Maynard et al. 2015). Coagulation, which has an important role in
597 the maintenance of hemostasis, is known to increase with age and contributes to the higher
598 incidence of cardiovascular diseases in the elderly (Franchini 2006; Khan et al. 2017). These
599 pathways overlap with recent findings from Kowalczyk et al. 2020, where they used the
600 number of AA substitutions on a phylogenetic branch to infer shifts associated with lifespan.
601 They found that pathways such as inflammation, DNA repair, cell death, the IGF1 pathway,
602 and immunity were under increased evolutionary constraint in large and long-lived
603 mammals.

604 We did not find a specific enrichment in aging-associated lists among the uncovered genes.
605 This might be explained by the fact that our analysis is intended to identify genes and
606 pathways that are shared across mammals, while most of the aging-related genes
607 discovered so far are mainly the result of single species approaches that capture genes
608 driving current variation within species rather than crucial changes fixed along the
609 phylogeny. However, many genes have been previously associated with longevity. A good
610 example is two AA changes in *WRN* gene that were validated in our study at positions 1018
611 and 1055, both in the RQC domain, which is crucial for DNA binding and for many protein
612 interactions (Tadokoro et al. 2012). *WRN* codifies for the Werner protein, which plays a
613 critical role in maintaining the structure and integrity of the DNA. More than 60 mutations in
614 the *WRN* gene are known to cause Werner's syndrome, which is characterized by
615 dramatically early appearance of features associated with aging. The two positions we
616 identified (g.31141514T>C and g.31141706A>G) have not been reported before, because

617 they show no variation in humans, suggesting a potential role of these specific positions in
618 the evolution of lifespan in mammals.

619 Four genes showed a significant relationship between LQ and root-to-tip τ (PGLS at
620 FDR<0.05): *TOR2A*, *ADCY7*, *CDK12* and *SPAG16*. Since they have co-evolved with
621 longevity patterns across mammals, these are very good candidates for future aging studies.
622 Some have been previously involved in regulating longevity-related pathways. For example,
623 *TOR2A* is a gene involved in cardiovascular diseases (Sun et al. 2020) included in a CNV
624 region in chromosome 9, correlating with longevity in a GWAS of Han Chinese individuals
625 (Zhao et al. 2018). *ADCY7* is a key gene in the longevity regulating pathway and was
626 recently associated with cancer mortality in dog breeds (Doherty et al. 2020). *CDK12* has
627 been observed to be required for stress activated gene expression (Li et al. 2016). In
628 contrast, *SPAG16* has not been previously associated with longevity. Overall, using both
629 approaches, we provide a list of genes that align with previous observations, but there are
630 also new longevity-associated genes and mutations that will need to be validated
631 experimentally.

632 *Limitations of the study*

633 We should acknowledge some limitations in our study. First, we analyzed a reduced number
634 of species and genes. Given the number of species and quality of gene alignments, we
635 could get genetic and phenotypic data for 57 mammals. Out of 19,170 genes, we evaluated
636 13,035 good-quality genes. Very recently, the genomes of 250 mammalian species,
637 including 132 assemblies, have been released (Zoonomia Consortium 2020), that resource
638 can eventually be used for analyses similar to the one presented here. However, acquisition
639 of high-quality samples was a major issue in that work (for instance, only 22 out of the 132
640 assemblies present contigs of N50 quality > 100Kbps) so the inclusion of these fragmented
641 genomes would impact the comprehensiveness of our study because of a drastic reduction
642 of the number of genes that we would be able to consistently analyze over all the phylogeny.
643 Second, our power to validate CAAS depends on the numbers of non-extreme species
644 showing either the long-lived or the short-lived amino acid residue. In some cases, the
645 long/short-lived amino acid identified was not present in any other mammal, or only in a few,
646 which made validation impossible. These cases are of course of interest, but beyond the
647 scope of the present work. Third, because the decile strategy was decided *a priori*, it is likely
648 that we have not explored the full set of AA changes that were involved in changes in
649 mammalian lifespan. However, Supplementary Figure 2 suggests that using more extreme
650 longevity values to classify CAAS may provide even more information of the genomic
651 architecture of lifespan. Fourth, in this study we used the short-lived mammal with the largest

652 available data on protein folding (rat and human), to demonstrate the level of stabilization of
653 the proteins coded by aging-related genes detected in this study. However, the comparison
654 was performed upon the reduced set of proteins with available folding data, which may not
655 be representative of the whole proteome. Finally, in the CAAS method we identified point
656 mutations that are ultimately assigned to genes. To study the heritability explained by these
657 genes we assigned to each gene all the SNPs lying in its coding region (plus a 5kb window).
658 This can introduce a bias because of complicated LD patterns and because many parts of
659 the gene might not be relevant even if a GWAS association is lying in the gene. However,
660 such bias would of course be conservative, even in cases where there is a GWAS signal
661 lying in a gene.

662 *Conclusions*

663 Our findings provide evidence on the genes and cellular mechanisms that may play a role in
664 regulating mammalian lifespan, strongly suggesting that protein stability is linked to
665 increased longevity and supporting an evolutionary trend towards longer lifespan in
666 mammals. Moreover, our study is the first to showcase how comparative-genomic studies
667 can illuminate the genetic architecture of human traits, including clinical and medical
668 phenotypes, and supports the use of comparative genomics studies to understand complex
669 human traits.

670

671 **Acknowledgements**

672 We thank T. Marquès-Bonet for his insights discussing the analyses. This work was
673 supported by: AEI-PGC2018-101927-BI00(FEDER/UE), the Spanish National Institute of
674 Bioinformatics of the Instituto de Salud Carlos III (PT17/0009/0020), FEDER (Fondo
675 Europeo de Desarrollo Regional)/FSE (Fondo Social Europeo), “Unidad de Excelencia María
676 de Maeztu”, funded by the AEI (CEX2018-000792-M) and Secretaria d’Universitats i
677 Recerca and CERCA Programme del Departament d’Economia i Coneixement de la
678 Generalitat de Catalunya (GRC 2017 SGR 880).

679

680 **Table 1.** Lists of discovered and validated CAAS and genes. Numbers in parentheses
681 represent the percentage of phylogenetically validated positions.

682

	Discovered		Validated RRPP	
	CAAS	Genes	CAAS	Genes
Scenario 1	284	273	131 (46.1%)	128
Scenario 2	2453	1822	1025 (41.8%)	891
Scenario 3	533	495	185 (33.5%)	182
Scenarios 1 + 2	2737	2004	1157 (42.3%)	996

683

684 **Figure Legends**

685

686 **Figure 1.** Workflow used in this study for the detection of Convergent Amino-Acid
687 Substitutions (CAAS). In the Discovery phase, we identified AA substitutions that were
688 exclusive from species in the top (yellow) and low (blue) deciles. In the Validation phase, we
689 classified the species from intermediate deciles (red) in two groups, the species having the
690 “long-lived” and the “short-lived” AA version. Finally, we ran a RRPP phylogenetic ANOVA to
691 validate each discovered AA, keeping as significant only those for which we validated the
692 direction of the effect (FDR<0.05).

693 **Figure 2.** (A) Manhattan plot of gene-based association results of the phylogenetically-
694 controlled regression (PGLS) for LQ. Each dot represents a gene and those depicted in red
695 represent significance at FDR<0.1. The negative logarithm of the FDR P-value for each
696 gene tested is reported on the y axis. P-value cutoffs corresponding to the Benjamini-
697 Hochberg threshold FDR=0.05 and FDR=0.1, based on the 17,969 genes tested, are
698 denoted by the dashed and dotted lines respectively. (B-E) Phylogenetically controlled
699 regression (PGLS) between log₁₀ root-to-tip ω for the significant genes (B) SPAG16, (C)
700 TOR2A, (D) ADCY7, and (E) CDK12 are displayed against log₁₀ LQ. Black lines represent
701 the regression slope of the linear model. UCSC version names were used for species
702 labeling. Correspondence to the species names can be found in Supplementary Table 1.

703 **Figure 3.** Stratified Q-Q plot for human longevity shows consistent enrichment across
704 several assessed gene sets. Annotation categories were i) all SNPs in the GWAS (orange);
705 ii) SNPs in genic regions of genes screened by the CAAS method (yellow); iii) SNPs in the
706 discovered genes (light blue); iv) SNPs in genes validated with RRPP (dark blue); and v)
707 SNPs in genes nominally significant ($P_{\text{cons}} < 0.05$) in the PGLS regression (green). All genic
708 regions were defined by gene boundaries plus 5Kb. The genes we validated in the study
709 were enriched in human longevity signal.

References

- 710 Adzhubei, Ivan A., Steffen Schmidt, Leonid Peshkin, Vasily E. Ramensky, Anna
711 Gerasimova, Peer Bork, Alexey S. Kondrashov, and Shamil R. Sunyaev. 2010. "A
712 Method and Server for Predicting Damaging Missense Mutations." *Nature Methods* 7
713 (4): 248–49. <https://doi.org/10.1038/nmeth0410-248>.
- 714 Austad, Steven N. 2005. "Diverse Aging Rates in Metazoans: Targets for Functional
715 Genomics." *Mechanisms of Ageing and Development*, Functional Genomics of
716 Ageing II, 126 (1): 43–49. <https://doi.org/10.1016/j.mad.2004.09.022>.
- 717 Austad, Steven N., and Kathleen E. Fischer. 1991. "Mammalian Aging, Metabolism, and
718 Ecology: Evidence From the Bats and Marsupials." *Journal of Gerontology* 46 (2):
719 B47–53. <https://doi.org/10.1093/geronj/46.2.B47>.
- 720 Baker, Joanna, Andrew Meade, Mark Pagel, and Chris Venditti. 2015. "Adaptive Evolution
721 toward Larger Size in Mammals." *Proceedings of the National Academy of Sciences*
722 *of the United States of America* 112 (16): 5093–98.
723 <https://doi.org/10.1073/pnas.1419823112>.
- 724 Boddy, Amy M., Peter W. Harrison, Stephen H. Montgomery, Jason A. Caravas, Mary Ann
725 Raghanti, Kimberley A. Phillips, Nicholas I. Mundy, and Derek E. Wildman. 2017.
726 "Evidence of a Conserved Molecular Response to Selection for Increased Brain Size
727 in Primates." *Genome Biology and Evolution* 9 (3): 700–713.
728 <https://doi.org/10.1093/gbe/evx028>.
- 729 Buffenstein, Rochelle. 2005. "The Naked Mole-Rat: A New Long-Living Model for Human
730 Aging Research." *The Journals of Gerontology: Series A* 60 (11): 1369–77.
731 <https://doi.org/10.1093/gerona/60.11.1369>.
- 732 Bullock, A. N., J. Henckel, B. S. DeDecker, C. M. Johnson, P. V. Nikolova, M. R. Proctor, D.
733 P. Lane, and A. R. Fersht. 1997. "Thermodynamic Stability of Wild-Type and Mutant
734 P53 Core Domain." *Proceedings of the National Academy of Sciences of the United*
735 *States of America* 94 (26): 14338–42. <https://doi.org/10.1073/pnas.94.26.14338>.
- 736 Buniello, Annalisa, Jacqueline A. L. MacArthur, Maria Cerezo, Laura W. Harris, James
737 Hayhurst, Cinzia Malangone, Aoife McMahon, et al. 2019. "The NHGRI-EBI GWAS
738 Catalog of Published Genome-Wide Association Studies, Targeted Arrays and
739 Summary Statistics 2019." *Nucleic Acids Research* 47 (D1): D1005–12.
740 <https://doi.org/10.1093/nar/gky1120>.
- 741 Buß, Oliver, Jens Rudat, and Katrin Ochsenreither. 2018. "FoldX as Protein Engineering
742 Tool: Better Than Random Based Approaches?" *Computational and Structural*
743 *Biotechnology Journal* 16: 25–33. <https://doi.org/10.1016/j.csbj.2018.01.002>.
- 744 Chikina, Maria, Joseph D. Robinson, and Nathan L. Clark. 2016. "Hundreds of Genes
745 Experienced Convergent Shifts in Selective Pressure in Marine Mammals." *Molecular*
746 *Biology and Evolution* 33 (9): 2182–92. <https://doi.org/10.1093/molbev/msw112>.
- 747 Collyer, Michael L., and Dean C. Adams. 2018. "RRPP: An r Package for Fitting Linear
748 Models to High-Dimensional Data Using Residual Randomization." *Methods in*
749 *Ecology and Evolution* 9 (7): 1772–79. <https://doi.org/10.1111/2041-210X.13029>.
- 750 DeCasien, Alex R., Scott A. Williams, and James P. Higham. 2017. "Primate Brain Size Is
751 Predicted by Diet but Not Sociality." *Nature Ecology & Evolution* 1 (5): 0112.
752 <https://doi.org/10.1038/s41559-017-0112>.
- 753 Deelen, Joris, Daniel S. Evans, Dan E. Arking, Niccolò Tesi, Marianne Nygaard, Xiaomin
754 Liu, Mary K. Wojczynski, et al. 2019. "A Meta-Analysis of Genome-Wide Association
755 Studies Identifies Multiple Longevity Genes." *Nature Communications* 10 (1): 1–14.
756 <https://doi.org/10.1038/s41467-019-11558-2>.
- 757 Doherty, Aoife, Inês Lopes, Christopher T. Ford, Gianni Monaco, Patrick Guest, and João
758 Pedro de Magalhães. 2020. "A Scan for Genes Associated with Cancer Mortality and
759 Longevity in Pedigree Dog Breeds." *Mammalian Genome* 31 (7): 215–27.
760 <https://doi.org/10.1007/s00335-020-09845-1>.

- 761 Finucane, Hilary K., Brendan Bulik-Sullivan, Alexander Gusev, Gosia Trynka, Yakir Reshef,
762 Po-Ru Loh, Verner Anttila, et al. 2015. "Partitioning Heritability by Functional
763 Annotation Using Genome-Wide Association Summary Statistics." *Nature Genetics*
764 47 (11): 1228–35. <https://doi.org/10.1038/ng.3404>.
- 765 Fontana, Luigi, and Linda Partridge. 2015. "Promoting Health and Longevity through Diet:
766 From Model Organisms to Humans." *Cell* 161 (1): 106–18.
767 <https://doi.org/10.1016/j.cell.2015.02.020>.
- 768 Foote, Andrew D., Yue Liu, Gregg W. C. Thomas, Tomáš Vinař, Jessica Alföldi, Jixin Deng,
769 Shannon Dugan, et al. 2015. "Convergent Evolution of the Genomes of Marine
770 Mammals." *Nature Genetics* 47 (3): 272–75. <https://doi.org/10.1038/ng.3198>.
- 771 Franchini, Massimo. 2006. "Hemostasis and Aging." *Critical Reviews in*
772 *Oncology/Hematology* 60 (2): 144–51.
773 <https://doi.org/10.1016/j.critrevonc.2006.06.004>.
- 774 Hekimi, S. 2003. "Genetics and the Specificity of the Aging Process." *Science* 299 (5611):
775 1351–54. <https://doi.org/10.1126/science.1082358>.
- 776 Herskind, A. M., M. McGue, N. V. Holm, T. I. Sørensen, B. Harvald, and J. W. Vaupel. 1996.
777 "The Heritability of Human Longevity: A Population-Based Study of 2872 Danish
778 Twin Pairs Born 1870-1900." *Human Genetics* 97 (3): 319–23.
779 <https://doi.org/10.1007/BF02185763>.
- 780 Huang, Zixia, Conor V. Whelan, Nicole M. Foley, David Jebb, Frédéric Touzalin, Eric J. Petit,
781 Sébastien J. Puechmaile, and Emma C. Teeling. 2019. "Longitudinal Comparative
782 Transcriptomics Reveals Unique Mechanisms Underlying Extended Healthspan in
783 Bats." *Nature Ecology & Evolution* 3 (7): 1110–20. <https://doi.org/10.1038/s41559-019-0913-3>.
- 784
- 785 Huelsenbeck, John P., Rasmus Nielsen, and Jonathan P. Bollback. 2003. "Stochastic
786 Mapping of Morphological Characters." *Systematic Biology* 52 (2): 131–58.
787 <https://doi.org/10.1080/10635150390192780>.
- 788 Jay, Jeremy J., and Cory Brouwer. 2016. "Lollipops in the Clinic: Information Dense Mutation
789 Plots for Precision Medicine." Edited by Jonathan H. Badger. *PLOS ONE* 11 (8):
790 e0160519. <https://doi.org/10.1371/journal.pone.0160519>.
- 791 Kaplanis, Joanna, Assaf Gordon, Tal Shor, Omer Weissbrod, Dan Geiger, Mary Wahl,
792 Michael Gershovits, et al. 2018. "Quantitative Analysis of Population-Scale Family
793 Trees with Millions of Relatives." *Science (New York, N.Y.)* 360 (6385): 171–75.
794 <https://doi.org/10.1126/science.aam9309>.
- 795 Karczewski, Konrad J., Laurent C. Francioli, Grace Tiao, Beryl B. Cummings, Jessica Alföldi,
796 Qingbo Wang, Ryan L. Collins, et al. 2020. "The Mutational Constraint Spectrum
797 Quantified from Variation in 141,456 Humans." *Nature* 581 (7809): 434–43.
798 <https://doi.org/10.1038/s41586-020-2308-7>.
- 799 Keane, Michael, Jeremy Semeiks, Andrew E. Webb, Yang I. Li, Víctor Quesada, Thomas
800 Craig, Lone Bruhn Madsen, et al. 2015. "Insights into the Evolution of Longevity from
801 the Bowhead Whale Genome." *Cell Reports* 10 (1): 112–22.
802 <https://doi.org/10.1016/j.celrep.2014.12.008>.
- 803 Khan, Sadiya S., Sanjiv J. Shah, Ekaterina Klyachko, Abigail S. Baldrige, Mesut Eren,
804 Aaron T. Place, Abraham Aviv, et al. 2017. "A Null Mutation in SERPINE1 Protects
805 against Biological Aging in Humans." *Science Advances* 3 (11): eaao1617.
806 <https://doi.org/10.1126/sciadv.aao1617>.
- 807 Kim, Eun Bae, Xiaodong Fang, Alexey A. Fushan, Zhiyong Huang, Alexei V. Lobanov, Lijuan
808 Han, Stefano M. Marino, et al. 2011. "Genome Sequencing Reveals Insights into
809 Physiology and Longevity of the Naked Mole Rat." *Nature* 479 (7372): 223–27.
810 <https://doi.org/10.1038/nature10533>.
- 811 Kowalczyk, Amanda, Raghavendran Partha, Nathan L. Clark, and Maria Chikina. 2020. "Pan-
812 Mammalian Analysis of Molecular Constraints Underlying Extended Lifespan." Edited
813 by Matt Kaeberlein and Diethard Tautz. *ELife* 9 (February): e51089.
814 <https://doi.org/10.7554/eLife.51089>.

- 815 Lamparter, David, Daniel Marbach, Rico Rueedi, Zoltán Kutalik, and Sven Bergmann. 2016.
816 “Fast and Rigorous Computation of Gene and Pathway Scores from SNP-Based
817 Summary Statistics.” *PLoS Computational Biology* 12 (1): e1004714.
818 <https://doi.org/10.1371/journal.pcbi.1004714>.
- 819 Li, Xuan, Nirmalya Chatterjee, Kerstin Spirohn, Michael Boutros, and Dirk Bohmann. 2016.
820 “Cdk12 Is A Gene-Selective RNA Polymerase II Kinase That Regulates a Subset of
821 the Transcriptome, Including Nrf2 Target Genes.” *Scientific Reports* 6 (1): 21455.
822 <https://doi.org/10.1038/srep21455>.
- 823 Liao, Yuxing, Jing Wang, Eric J. Jaehnig, Zhiao Shi, and Bing Zhang. 2019. “WebGestalt
824 2019: Gene Set Analysis Toolkit with Revamped UIs and APIs.” *Nucleic Acids
825 Research* 47 (W1): W199–205. <https://doi.org/10.1093/nar/gkz401>.
- 826 Liberzon, Arthur, Chet Birger, Helga Thorvaldsdóttir, Mahmoud Ghandi, Jill P. Mesirov, and
827 Pablo Tamayo. 2015. “The Molecular Signatures Database (MSigDB) Hallmark Gene
828 Set Collection.” *Cell Systems* 1 (6): 417–25.
829 <https://doi.org/10.1016/j.cels.2015.12.004>.
- 830 López-Otín, Carlos, Maria A. Blasco, Linda Partridge, Manuel Serrano, and Guido Kroemer.
831 2013. “The Hallmarks of Aging.” *Cell* 153 (6): 1194–1217.
832 <https://doi.org/10.1016/j.cell.2013.05.039>.
- 833 Lyson, T. R., I. M. Miller, A. D. Bercovici, K. Weissenburger, A. J. Fuentes, W. C. Clyde, J.
834 W. Hagadorn, et al. 2019. “Exceptional Continental Record of Biotic Recovery after
835 the Cretaceous–Paleogene Mass Extinction.” *Science* 366 (6468): 977–83.
836 <https://doi.org/10.1126/science.aay2268>.
- 837 Ma, Siming, and Vadim N. Gladyshev. 2017. “Molecular Signatures of Longevity: Insights
838 from Cross-Species Comparative Studies.” *Seminars in Cell & Developmental
839 Biology* 70 (October): 190–203. <https://doi.org/10.1016/j.semcdb.2017.08.007>.
- 840 Magalhães, João Pedro de, Joana Costa, and George M. Church. 2007. “An Analysis of the
841 Relationship Between Metabolism, Developmental Schedules, and Longevity Using
842 Phylogenetic Independent Contrasts.” *The Journals of Gerontology. Series A,
843 Biological Sciences and Medical Sciences* 62 (2): 149–60.
- 844 Magalhães, João Pedro de, and Jingwei Wang. 2019. “The Fog of Genetics: What Is Known,
845 Unknown and Unknowable in the Genetics of Complex Traits and Diseases.” *EMBO
846 Reports* 20 (11): e48054. <https://doi.org/10.15252/embr.201948054>.
- 847 Maynard, Scott, Evandro Fei Fang, Morten Scheibye-Knudsen, Deborah L. Croteau, and
848 Vilhelm A. Bohr. 2015. “DNA Damage, DNA Repair, Aging, and Neurodegeneration.”
849 *Cold Spring Harbor Perspectives in Medicine* 5 (10).
850 <https://doi.org/10.1101/cshperspect.a025130>.
- 851 McLaren, William, Laurent Gil, Sarah E. Hunt, Harpreet Singh Riat, Graham R. S. Ritchie,
852 Anja Thormann, Paul Flicek, and Fiona Cunningham. 2016. “The Ensembl Variant
853 Effect Predictor.” *Genome Biology* 17 (1): 122. <https://doi.org/10.1186/s13059-016-0974-4>.
- 854
- 855 Montgomery, Stephen H., and Nicholas I. Mundy. 2012. “Evolution of *Aspm* Is Associated
856 with Both Increases and Decreases in Brain Size in Primates.” *Evolution* 66 (3): 927–
857 32. <https://doi.org/10.1111/j.1558-5646.2011.01487.x>.
- 858 Muntané, Gerard, Xavier Farré, Juan Antonio Rodríguez, Cinta Pegueroles, David A.
859 Hughes, João Pedro de Magalhães, Toni Gabaldón, and Arcadi Navarro. 2018.
860 “Biological Processes Modulating Longevity across Primates: A Phylogenetic
861 Genome-Phenome Analysis.” *Molecular Biology and Evolution* 35 (8): 1990–2004.
862 <https://doi.org/10.1093/molbev/msy105>.
- 863 Myers, P, R Espinosa, C. S Parr, T Jones, G. S Hammond, and T. A Dewey. 2019. “The
864 Animal Diversity Web (Online).”
- 865 Ng, Pauline C., and Steven Henikoff. 2003. “SIFT: Predicting Amino Acid Changes That
866 Affect Protein Function.” *Nucleic Acids Research* 31 (13): 3812–14.
867 <https://doi.org/10.1093/nar/gkg509>.

- 868 O'Leary, Maureen A., Jonathan I. Bloch, John J. Flynn, Timothy J. Gaudin, Andres
869 Giallombardo, Norberto P. Giannini, Suzann L. Goldberg, et al. 2013. "The Placental
870 Mammal Ancestor and the Post-K-Pg Radiation of Placentals." *Science* 339 (6120):
871 662–67. <https://doi.org/10.1126/science.1229237>.
- 872 Orme, David. 2018. "The Caper Package: Comparative Analysis of Phylogenetics and
873 Evolution in R," April. [https://cran.r-
874 project.org/web/packages/caper/vignettes/caper.pdf](https://cran.r-project.org/web/packages/caper/vignettes/caper.pdf).
- 875 Pérez, Viviana I., Rochelle Buffenstein, Venkata Masamsetti, Shanique Leonard, Adam B.
876 Salmon, James Mele, Blazej Andziak, et al. 2009. "Protein Stability and Resistance
877 to Oxidative Stress Are Determinants of Longevity in the Longest-Living Rodent, the
878 Naked Mole-Rat." *Proceedings of the National Academy of Sciences of the United
879 States of America* 106 (9): 3059–64. <https://doi.org/10.1073/pnas.0809620106>.
- 880 Pickrell, John. 2019. "How the Earliest Mammals Thrived alongside Dinosaurs." *Nature* 574
881 (7779): 468–72. <https://doi.org/10.1038/d41586-019-03170-7>.
- 882 Pomeroy, Derek. 1990. "Why Fly? The Possible Benefits for Lower Mortality." *Biological
883 Journal of the Linnean Society* 40 (1): 53–65. [https://doi.org/10.1111/j.1095-
8312.1990.tb00534.x](https://doi.org/10.1111/j.1095-
884 8312.1990.tb00534.x).
- 885 Powers, Evan T., Richard I. Morimoto, Andrew Dillin, Jeffery W. Kelly, and William E. Balch.
886 2009. "Biological and Chemical Approaches to Diseases of Proteostasis Deficiency." *Annual Review of Biochemistry* 78: 959–91.
887 <https://doi.org/10.1146/annurev.biochem.052308.114844>.
- 888 Ratikainen, Irja I., and Hanna Kokko. 2019. "The Coevolution of Lifespan and Reversible
889 Plasticity." *Nature Communications* 10 (1): 538. [https://doi.org/10.1038/s41467-019-
891 08502-9](https://doi.org/10.1038/s41467-019-
890 08502-9).
- 892 Rentzsch, Philipp, Daniela Witten, Gregory M. Cooper, Jay Shendure, and Martin Kircher.
893 2019. "CADD: Predicting the Deleteriousness of Variants throughout the Human
894 Genome." *Nucleic Acids Research* 47 (D1): D886–94.
895 <https://doi.org/10.1093/nar/gky1016>.
- 896 Revell, Liam J. 2012. "Phytools: An R Package for Phylogenetic Comparative Biology (and
897 Other Things): *Phytools: R Package*." *Methods in Ecology and Evolution* 3 (2): 217–
898 23. <https://doi.org/10.1111/j.2041-210X.2011.00169.x>.
- 899 Rice, P., I. Longden, and A. Bleasby. 2000. "EMBOSS: The European Molecular Biology
900 Open Software Suite." *Trends in Genetics: TIG* 16 (6): 276–77.
901 [https://doi.org/10.1016/s0168-9525\(00\)02024-2](https://doi.org/10.1016/s0168-9525(00)02024-2).
- 902 Rose, Peter W., Andreas Prlić, Ali Altunkaya, Chunxiao Bi, Anthony R. Bradley, Cole H.
903 Christie, Luigi Di Costanzo, et al. 2017. "The RCSB Protein Data Bank: Integrative
904 View of Protein, Gene and 3D Structural Information." *Nucleic Acids Research* 45
905 (D1): D271–81. <https://doi.org/10.1093/nar/gkw1000>.
- 906 Ruby, J Graham, Megan Smith, and Rochelle Buffenstein. 2018. "Naked Mole-Rat Mortality
907 Rates Defy Gompertzian Laws by Not Increasing with Age." Edited by Michael Rose.
908 *ELife* 7: e31157. <https://doi.org/10.7554/eLife.31157>.
- 909 Ruby, J. Graham, Kevin M. Wright, Kristin A. Rand, Amir Kermany, Keith Noto, Don Curtis,
910 Neal Varner, et al. 2018. "Estimates of the Heritability of Human Longevity Are
911 Substantially Inflated Due to Assortative Mating." *Genetics* 210 (3): 1109–24.
912 <https://doi.org/10.1534/genetics.118.301613>.
- 913 Santra, Mantu, Ken A. Dill, and Adam M. R. de Graff. 2019. "Proteostasis Collapse Is a
914 Driver of Cell Aging and Death." *Proceedings of the National Academy of Sciences*
915 116 (44): 22173–78. <https://doi.org/10.1073/pnas.1906592116>.
- 916 Sebastiani, Paola, and Thomas T. Perls. 2012. "The Genetics of Extreme Longevity:
917 Lessons from the New England Centenarian Study." *Frontiers in Genetics* 3: 277.
918 <https://doi.org/10.3389/fgene.2012.00277>.
- 919 Seim, Inge, Xiaodong Fang, Zhiqiang Xiong, Alexey V. Lobanov, Zhiyong Huang, Siming
920 Ma, Yue Feng, et al. 2013. "Genome Analysis Reveals Insights into Physiology and

- 921 Longevity of the Brandt's Bat *Myotis Brandtii*." *Nature Communications* 4 (1): 2212.
922 <https://doi.org/10.1038/ncomms3212>.
- 923 Shattuck, Milena R., and Scott A. Williams. 2010. "Arboreality Has Allowed for the Evolution
924 of Increased Longevity in Mammals." *Proceedings of the National Academy of
925 Sciences of the United States of America* 107 (10): 4635–39.
926 <https://doi.org/10.1073/pnas.0911439107>.
- 927 Speakman, John R. 2005. "Correlations between Physiology and Lifespan--Two Widely
928 Ignored Problems with Comparative Studies." *Aging Cell* 4 (4): 167–75.
929 <https://doi.org/10.1111/j.1474-9726.2005.00162.x>.
- 930 Sun, Shuo, Feng Zhang, Yan Pan, Yu Xu, Aidong Chen, Jian Wang, Haiyang Tang, and
931 Ying Han. 2020. "A TOR2A Gene Product: Salusin- β Contributes to Attenuated
932 Vasodilatation of Spontaneously Hypertensive Rats." *Cardiovascular Drugs and
933 Therapy*, May. <https://doi.org/10.1007/s10557-020-06983-1>.
- 934 Tacutu, Robi, Daniel Thornton, Emily Johnson, Arie Budovsky, Diogo Barardo, Thomas
935 Craig, Eugene Diana, et al. 2018. "Human Ageing Genomic Resources: New and
936 Updated Databases." *Nucleic Acids Research* 46 (D1): D1083–90.
937 <https://doi.org/10.1093/nar/gkx1042>.
- 938 Tian, Xiao, Andrei Seluanov, and Vera Gorbunova. 2017. "Molecular Mechanisms
939 Determining Lifespan in Short- and Long-Lived Species." *Trends in Endocrinology
940 and Metabolism: TEM* 28 (10): 722–34. <https://doi.org/10.1016/j.tem.2017.07.004>.
- 941 Timmers, Paul RHJ, Ninon Mounier, Kristi Lall, Krista Fischer, Zheng Ning, Xiao Feng,
942 Andrew D Bretherick, et al. 2019. "Genomics of 1 Million Parent Lifespans Implicates
943 Novel Pathways and Common Diseases and Distinguishes Survival Chances." *ELife*
944 8: e39856. <https://doi.org/10.7554/eLife.39856>.
- 945 Treaster, S. B., I. D. Ridgway, C. A. Richardson, M. B. Gaspar, A. R. Chaudhuri, and S. N.
946 Austad. 2014. "Superior Proteome Stability in the Longest Lived Animal." *Age
947 (Dordrecht, Netherlands)* 36 (3): 9597. <https://doi.org/10.1007/s11357-013-9597-9>.
- 948 Wang, Hui, Hanbo Zhao, Keping Sun, Xiaobin Huang, Longru Jin, and Jiang Feng. 2020.
949 "Evolutionary Basis of High-Frequency Hearing in the Cochleae of Echolocators
950 Revealed by Comparative Genomics." *Genome Biology and Evolution* 12 (1): 3740–
951 53. <https://doi.org/10.1093/gbe/evz250>.
- 952 Watanabe, Kyoko, Sven Stringer, Aleksandr Frei, Maša Umičević Mirkov, Christiaan de
953 Leeuw, Tinca J. C. Polderman, Sophie van der Sluis, Ole A. Andreassen, Benjamin
954 M. Neale, and Danielle Posthuma. 2019. "A Global Overview of Pleiotropy and
955 Genetic Architecture in Complex Traits." *Nature Genetics* 51 (9): 1339–48.
956 <https://doi.org/10.1038/s41588-019-0481-0>.
- 957 Webb, Benjamin, and Andrej Sali. 2016. "Comparative Protein Structure Modeling Using
958 MODELLER." *Current Protocols in Bioinformatics* 54: 5.6.1-5.6.37.
959 <https://doi.org/10.1002/cpbi.3>.
- 960 Yang, Z. 1997. "PAML: A Program Package for Phylogenetic Analysis by Maximum
961 Likelihood." *Computer Applications in the Biosciences: CABIOS* 13 (5): 555–56.
- 962 Zenin, Aleksandr, Yakov Tsepilov, Sodbo Sharapov, Evgeny Getmantsev, L. I. Menshikov,
963 Peter O. Fedichev, and Yurii Aulchenko. 2019. "Identification of 12 Genetic Loci
964 Associated with Human Healthspan." *Communications Biology* 2.
965 <https://doi.org/10.1038/s42003-019-0290-0>.
- 966 Zhang, Guojie, Cai Li, Qiye Li, Bo Li, Denis M. Larkin, Chul Lee, Jay F. Storz, et al. 2014.
967 "Comparative Genomics Reveals Insights into Avian Genome Evolution and
968 Adaptation." *Science (New York, N.Y.)* 346 (6215): 1311–20.
969 <https://doi.org/10.1126/science.1251385>.
- 970 Zhao, Xin, Xiaomin Liu, Aiping Zhang, Huashuai Chen, Qing Huo, Weiyang Li, Rui Ye, et al.
971 2018. "The Correlation of Copy Number Variations with Longevity in a Genome-Wide
972 Association Study of Han Chinese." *Aging (Albany NY)* 10 (6): 1206–22.
973 <https://doi.org/10.18632/aging.101461>.

- 974 Zhou, Wanding, Tenghui Chen, Zechen Chong, Mary A. Rohrdanz, James M. Melott, Chris
975 Wakefield, Jia Zeng, et al. 2015. "TransVar: A Multilevel Variant Annotator for
976 Precision Genomics." *Nature Methods* 12 (11): 1002–3.
977 <https://doi.org/10.1038/nmeth.3622>.
978 Zoonomia Consortium. 2020. "A Comparative Genomics Multitool for Scientific Discovery
979 and Conservation." *Nature* 587 (7833): 240–45. [https://doi.org/10.1038/s41586-020-](https://doi.org/10.1038/s41586-020-2876-6)
980 [2876-6](https://doi.org/10.1038/s41586-020-2876-6).
981

Figure 1

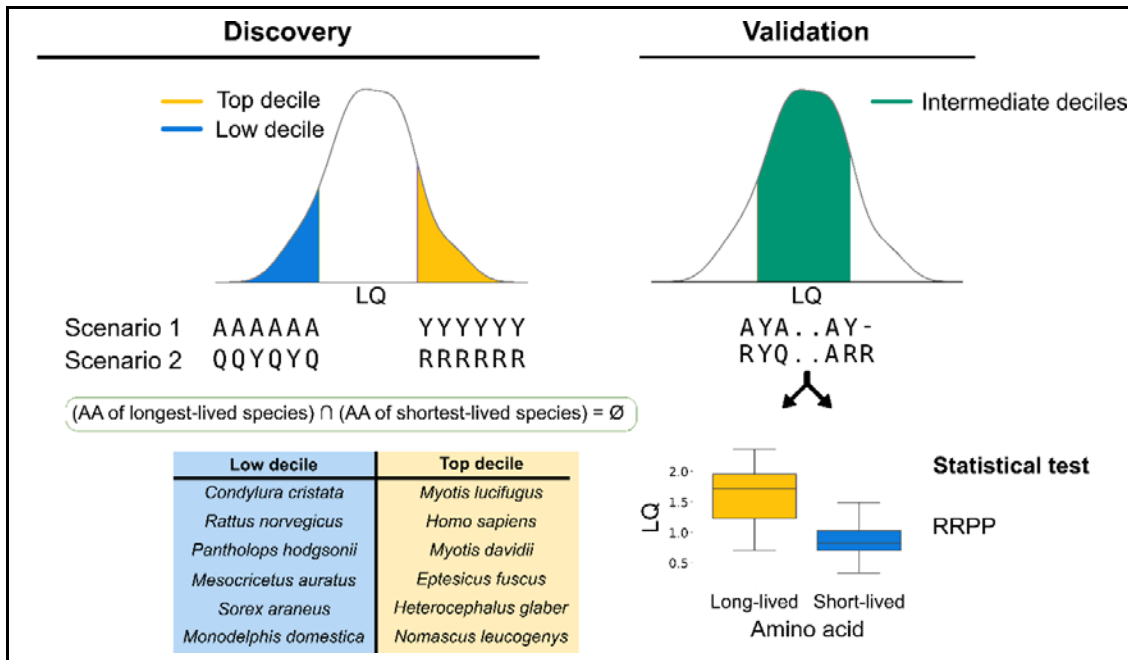


Figure 1. Workflow used in this study for the detection of Convergent Amino-Acid Substitutions (CAAS). In the Discovery phase, we identified AA substitutions that were exclusive from species in the top (yellow) and low (blue) deciles. In the Validation phase, we classified the species from intermediate deciles (red) in two groups, the species having the “long-lived” and the “short-lived” AA version. Finally, we ran a RRPP phylogenetic ANOVA to validate each discovered AA, keeping as significant only those for which we validated the direction of the effect (FDR<0.05).

Figure 2

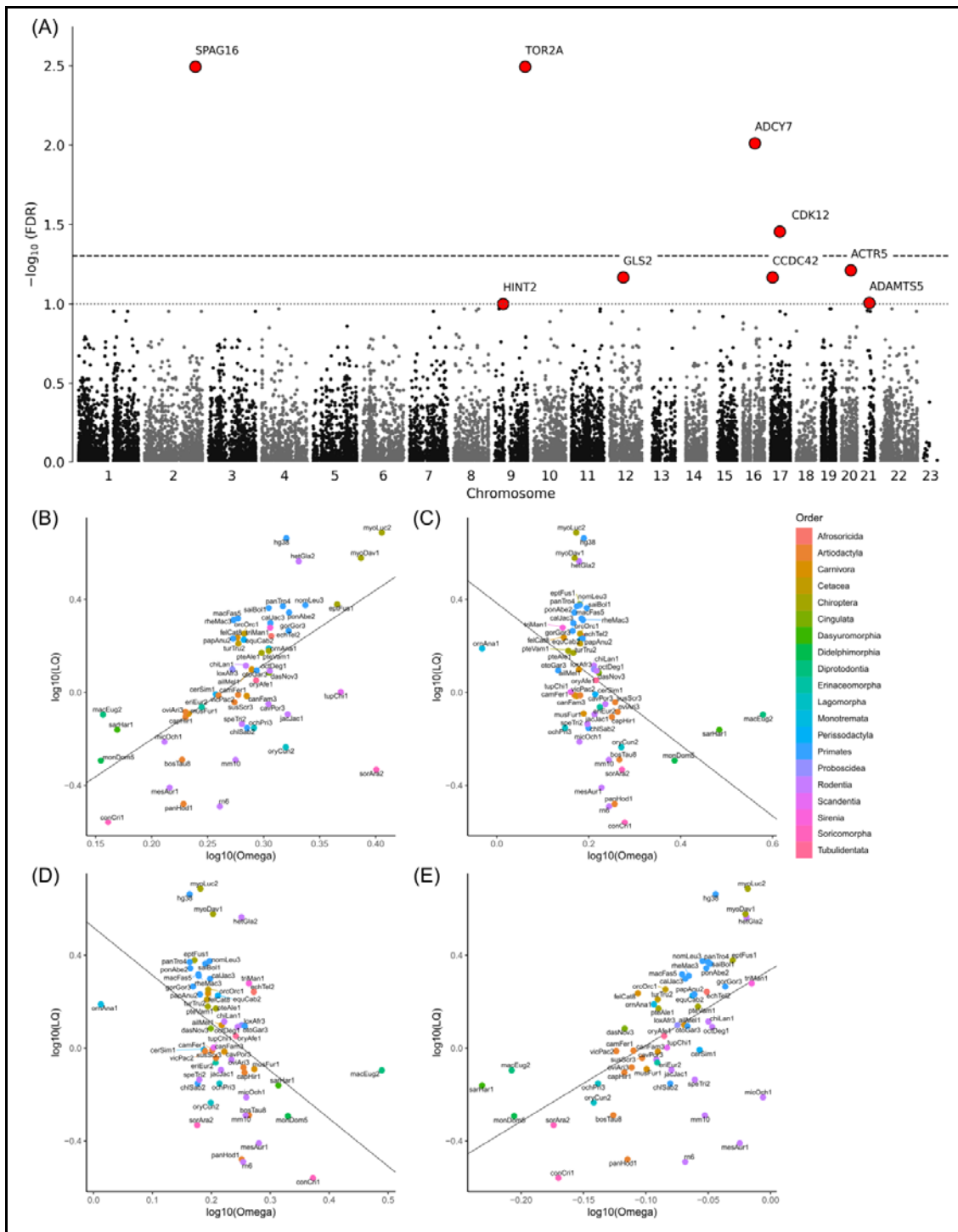


Figure 2. (A) Manhattan plot of gene-based association results of the phylogenetically-controlled regression (PGLS) for LQ. Each dot represents a gene and those depicted in red represent significance at $\text{FDR} < 0.1$. The negative logarithm of the FDR P-value for each gene tested is reported on the y axis. P-value cutoffs corresponding to the Benjamini-Hochberg threshold $\text{FDR} = 0.05$ and $\text{FDR} = 0.1$, based on the 17,969 genes

tested, are denoted by the dashed and dotted lines respectively. (B-E) Phylogenetically controlled regression (PGLS) between \log_{10} root-to-tip ω for the significant genes (B) SPAG16, (C) TOR2A, (D) ADCY7, and (E) CDK12 are displayed against \log_{10} LQ. Black lines represents the regression slope of the linear model. UCSC version names were used for species labeling. Correspondence to the species names can be found in Supplementary Table 1.

Figure 3

